Technical Sciences, 2025, 28, 199–213

UNIWERSYTET WARMIŃSKO-MAZURSKI W OLSZTYNIE

Yearbook peer-reviewed scientific journal
ISSN 1505-4675
e-ISSN 2083-4527
TECHNICAL SCIENCES
Homepage: https://czasopisma.uwm.edu.pl/index.php/ts/

DOI: https://doi.org/10.31648/ts.11552

FINITE ELEMENT ANALYSIS OF THE EIGENFREQUENCIES OF A MILLING MACHINE SUPPORT STRUCTURE

***Radosław Ciemierkiewicz*[1], *Bogusław Ładecki*[2]**

[1]ORCID: 0000-0002-3692-119X
[2]ORCID: 0000-0002-0281-2526
Faculty of Mechanical Engineering and Robotics
AGH University of Krakow

Received 18 June 2025, accepted 30 October 2025, available online 12 December 2025

K e y w o r d s: support structure of a milling machine, FE analysis, parametric optimization.

A b s t r a c t

The publication concerns the selection of dimensions for two support structure models of a woodworking spindle moulder, based on the results of finite element analyses: static structural and modal. Using the ANSYS Workbench software, a linear-elastic material behavior was assumed, and preliminary models of the milling machine frame and housing were analyzed, each assigned a different material – structural steel (S235JR) and gray cast iron (EN-GJL-250), respectively. After completing the Design and Analysis of Computer Experiments stage, optimization was carried out using ANSYS Workbench algorithms: the Response Surface Method and the Direct Optimization Method. As a result, the optimal geometric dimensions of the milling machine's support structures were identified, satisfying both strength and modal criteria.

Introduction

Finite element analysis (FE analysis) enables the approximate determination of results even for highly complex structures, for which obtaining exact solutions is difficult or economically unfeasible (SAVA et al. 2021, ZIENKIEWICZ, TAYLOR

Correspondence: Radosław Ciemierkiewicz, Department of Machine Design and Maintenance, AGH University of Krakow, al. Adama Mickiewicza 30, 30-059 Krakow, e mail: ciemierkiewicz@agh.edu.pl

2002). Modern simulation software makes it possible to model various phenomena related to machine operation, which helps improve the design of technical systems (QIU et al. 2018). FEM-based tools, particularly for studying structural vibrations, are especially important (CHAN et al. 2023, XI et al. 2019, DIKMEN et al. 2009). FE models of real-world systems are discrete systems with a finite number of degrees of freedom. In vibration analysis of such systems, the dynamic equation of motion can be applied (DONG et al. 2023). Expressed in matrix form, for a system with n degrees of freedom, it takes the form (1):

$$[M]\{\ddot{q}\} + [C]\{\dot{q}\} + [K]\{q\} = \{F(t)\} \tag{1}$$

where:

$[M]$ – mass matrix,
$\{\ddot{q}\}$ – nodal acceleration vector,
$[C]$ – damping matrix,
$\{\dot{q}\}$ – nodal velocity vector,
$[K]$ – stiffness matrix,
$[q]$ – nodal displacement vector,
$\{F(t)\}$ – nodal external force vector.

If the external force vector $\{F(t)\}$ in Equation (1) is equal to zero, the vibrations described by this equation are referred to as free vibrations (SZMIDLA, KLUBA 2011). Free vibration is the motion of a body caused by its displacement from a stable equilibrium position, occurring in the absence of external forces – except those that define the equilibrium and restore it. In the absence of significant damping, the system is typically analyzed in terms of natural vibrations (HERZ, NORDMANN 2020, GÉRADIN et al. 2015).

Modal analysis using computer-based methods is one of the approaches to studying natural vibrations (PEDRAMMEHR et al. 2011), used alongside classical analytical methods (JAROSZEWICZ et al. 2018, JAROSZEWICZ et al. 2017, JAROSZEWICZ, ZORYJ 1994). As a result of such analysis, key vibration characteristics are obtained: the natural frequencies and mode shapes of the system (QIU et al. 2018). These analyses can be performed at early stages of the design process, prior to defining and implementing more accurate damping-related parameters of the system. Modal analysis is recommended and often necessary for technical systems such as machine tools (LIU et al. 2022, DUNAJ et al. 2019). Vibrations generated during their operation affect not only the quality of machining, but also the service life of machine components (SHIHAN et al. 2020, VERVAEKE et al. 2019). A major factor contributing to reduced service life is mechanical resonance. The risk of resonance is evaluated by comparing the natural frequencies of the structure with the frequencies of vibrations induced by external excitations (CHAN et al. 2023, PEDRAMMEHR et al. 2011). Modal analysis is therefore a practical and valuable tool in the machine design process, allowing improvements to prototype designs and, most importantly, reducing the risk of resonance. It is also applied in diagnostics to identify potential resonance issues, including noise, reduced component life, or early system failures.

Using ANSYS Workbench, finite element models of the support structures of two types of milling machines were developed and analyzed using static structural and modal analysis (Fig. 1). The first machine (Fig. 2a) represents a commercial design, typical for professional woodworking stations used in large-scale production of functional parts. Milling machines with this type of support structure are heavy and equipped with components that facilitate the machining process. The second category includes non-professional designs, with frames made from joined profile sections – usually welded and bolted (Fig. 2b). Milling machines with this type of support structure feature relatively

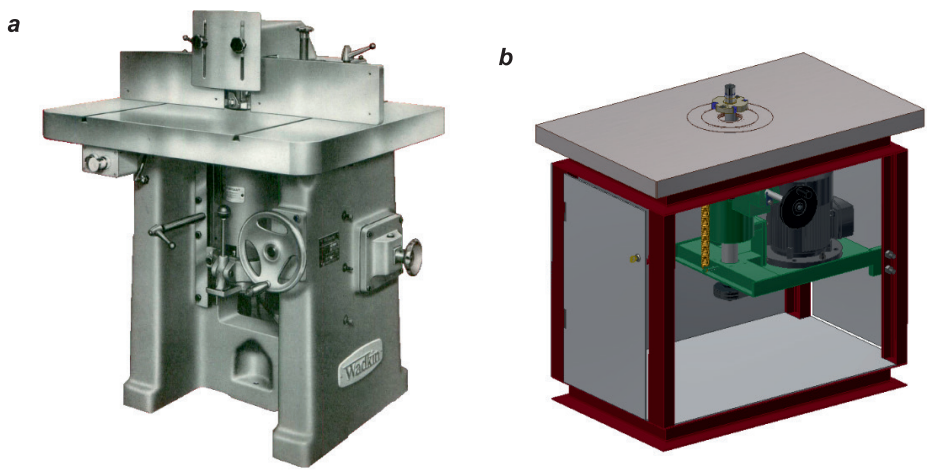

Fig. 1. Support structures of two types of woodworking milling machines analyzed: a) commercial, b) prototype (amateur-built)

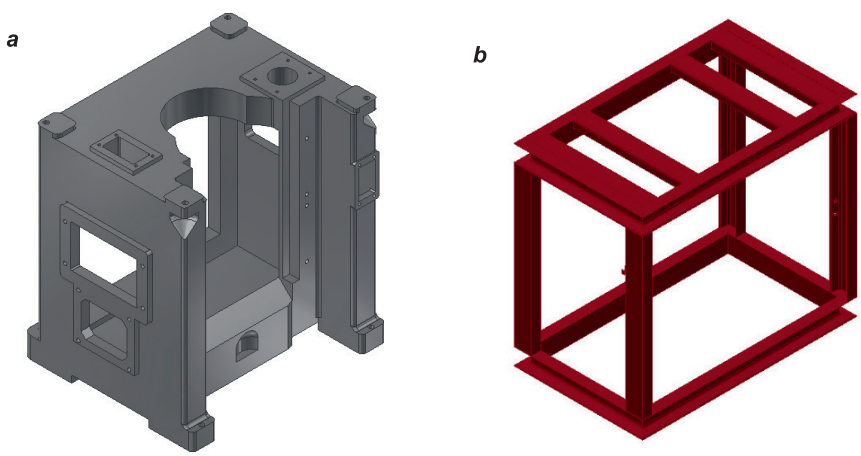

Fig. 2. Geometrical models of support structures for two types of milling machines used in FE analyses: a) commercial cast housing, b) prototype frame made of structural profiles

simple design solutions and their spare parts are usually cheaper and more readily available compared to those used in commercial machines. The frames in non-professional designs are sufficient for less demanding machining tasks, where high precision is not required.

The purpose of the analysis was to select the geometric dimensions of the support structures for two types of woodworking milling machines so that their first natural frequencies stayed at a specified level. The geometric models used for FE analyses are shown in Figure 2. The analysis also aimed to determine whether a more expensive cast frame offers better properties than a cheaper structure made of channel profiles, based on basic strength and modal criteria. The tools available in ANSYS Workbench – including the FE solver, the DesignXplorer module for designing computer experiments, and parametric optimization algorithms – were used to define the initial dimensions of the proposed structures.

Methods

An isotropic linear-elastic material model was assumed for all analyzed geometries in the simulations. The housing is made of gray cast iron EN-GJL-250, while the frame is made of structural steel S235JR. In the FE analysis, the welded structural profiles forming the frame were interconnected using the Share Topology feature provided in ANSYS SpaceClaim. The mechanical properties of both structures are listed in Tables 1 and 2, respectively.

Table 1

Material properties assumed for housing (material: EN-GJL-250)

Material parameter name	Symbol	Value	Unit
Young's modulus	E	110000	(MPa)
Density	$\boldsymbol{\rho}$	7200	(kg/m^3)
Tensile yield strength	R_e	250	(MPa)
Poisson's ratio	$\boldsymbol{\nu}$	0.28	

Table 2

Material properties assumed for frame (material: S235JR)

Material parameter name	Symbol	Value	Unit
Young's modulus	E	210000	(MPa)
Density	$\boldsymbol{\rho}$	8000	(kg/m^3)
Tensile yield strength	R_e	235	(MPa)
Poisson's ratio	$\boldsymbol{\nu}$	0.3	

The process considered in the design calculations is down milling using a straight-tooth cutter. During this process, a resultant cutting force is generated $\bar{F}$ (Fig. 3), which can be decomposed into one of two pairs of component forces: the radial force $\bar{F}_r$ and the tangential force $\bar{F}_v$ or the passive force $\bar{F}_p$ and the feed $\bar{F}_f$ force (GOLI et al. 2010). Since a straight-tooth cutter is assumed, no axial force is considered, which would typically appear when using a helical-tooth cutter.

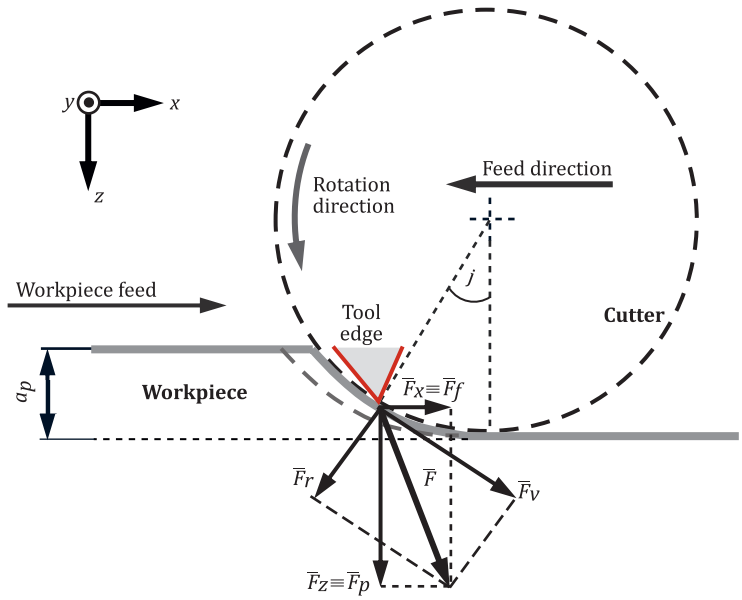

Fig. 3. Assumed force distribution in FE simulations of down milling using a straight-tooth cutter

Table 3 presents the values of the forces exerted by the workpiece material (wood) on the cutting tool, as well as the value of the force $\bar{Q}$ generated in the drive unit, resulting from the operation of the milling machine's belt-driven transmission system (see Fig. 4). In both the static structural and modal analyses, the masses of the components forming the equipment of the analyzed milling machines were taken into account. For geometrically complex components, simplified representations in the form of deformable point masses were applied. The mass values assigned to these point masses, which transfer loads through the structural support points, are listed in Table 4. The introduced point masses did not account for the mass moments of inertia of the components they represented. The total mass of all elements in the model with the cast housing was 1083.3 kg, while in the frame-based model it was 368.3 kg.

Table 3

Summary of forces adopted in the FE simulations

Symbol	Description	Value (N)
$\bar{F}$	Resultant cutting force (total)	255.3
$\bar{F}_x \equiv \bar{F}_f$	Cutting force – x component (feed direction)	142.3
$\bar{F}_z \equiv \bar{F}_p$	Cutting force – z component (passive direction)	212
$\bar{F}_r$	Radial cutting force	94.8
$\bar{F}_v$	Tangential cutting force	237.1
$\bar{Q}$	Resultant force generated by the drive unit	500

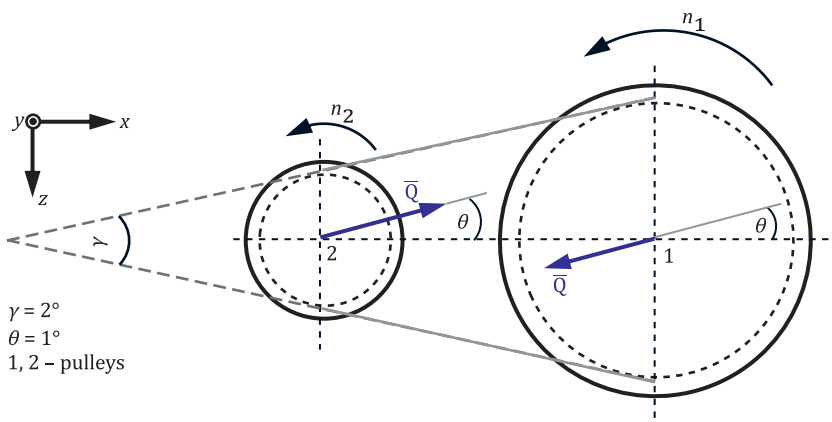

Fig. 4. Force scheme assumed in FE simulations for the V-belt transmission system

Table 4

Component masses considered in the FE simulations

Point mass	Description	Mass (kg)
m_1	side cover (prototype frame model)	5.5
m_2	front/rear cover (prototype frame model)	11.3
m_3	bottom cover (prototype frame model)	8.4
m_4	left side of the drive system (prototype frame model)	27.2
m_5	right side of the drive system (prototype frame model)	40
m_6	left side of the drive system (commercial housing model)	27.2
m_7	right side of the drive system (commercial housing model)	40

To evaluate the potential for resonance in the analyzed structures, the natural frequencies obtained from the FE analyses were compared with the excitation frequencies f_z, calculated using Equation (2) for three different rotational speeds of the cutting tool. The resulting excitation angular velocities and frequencies are

listed in Table 5. Based on the assumed spindle speeds (1800, 2500, 3000 RPM), the tool completes 30, 41, or 50 full rotations per second, depending on the simulation variant.

$$f_z = \frac{\omega}{2\pi} = \frac{n}{60} \tag{2}$$

where:

ω – angular velocity of the cutting tool,

n – rotational velocity of the cutting tool.

Table 5

Cutting tool parameters assumed and derived for down-milling of wood

Rotational speed n (RPM)	Angular velocity $\boldsymbol{\omega}$ (rad/s)	Excitation frequency f (Hz)
1800	188.5	30
2500	261.8	41.7
3000	314.2	50

The critical loading cases – identified as the most unfavorable from a strength perspective – are shown in Figure 5a for the housing and in Figure 5b for the frame. Point masses not labeled in the figures were applied at the center of gravity of the assemblies they represent. In the simulations, *Fixed Support* constraints were applied to the edges or surfaces of holes located near the base of the structure. The vector $\bar{g}$ shown in the figures represents gravitational acceleration (g = 9.8061 m/s^2). When determining the critical load scenarios, different load distributions acting on the supporting structures were considered.

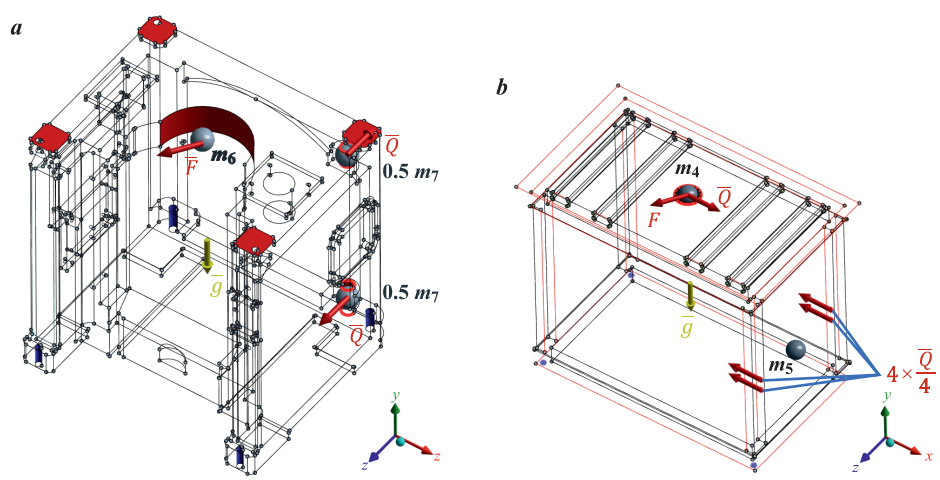

Fig. 5. Critical load cases assumed in the FE analyses for a) the housing, b) the frame model

The critical load case was identified based on the maximum total deformation and equivalent von Mises stress. Contour plots for the critical load case are shown in Figures 6–7 (total deformation of the housing and the frame) and Figures 8–9 (equivalent von Mises stress of the housing and the frame).

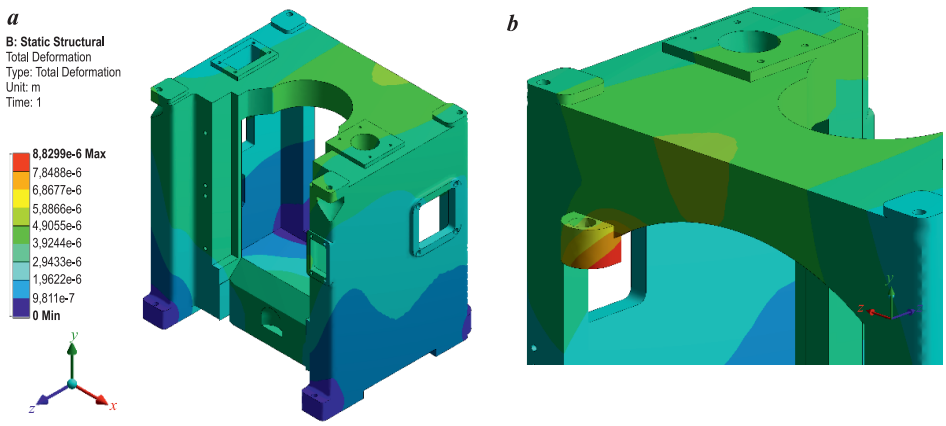

Fig. 6. Total deformation contour plot obtained for the critical load case of the housing model: a) overall view, b) area of maximum total deformation (detailed view)

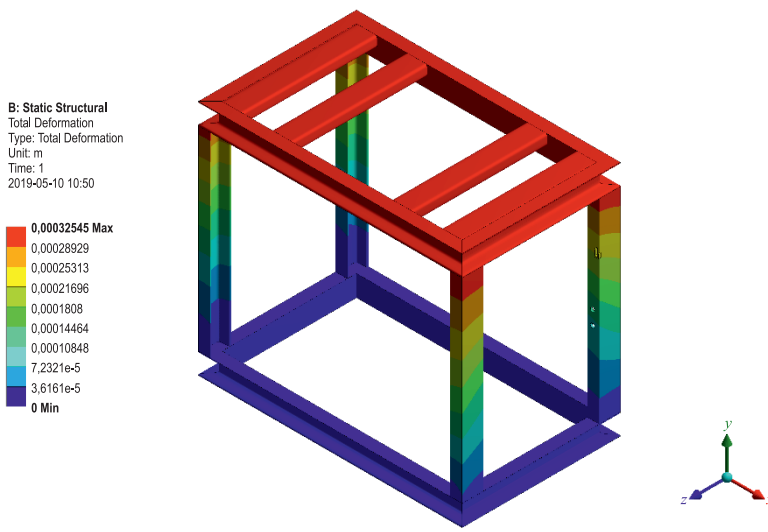

Fig. 7. Total deformation contour plot obtained for the critical load case of the frame model

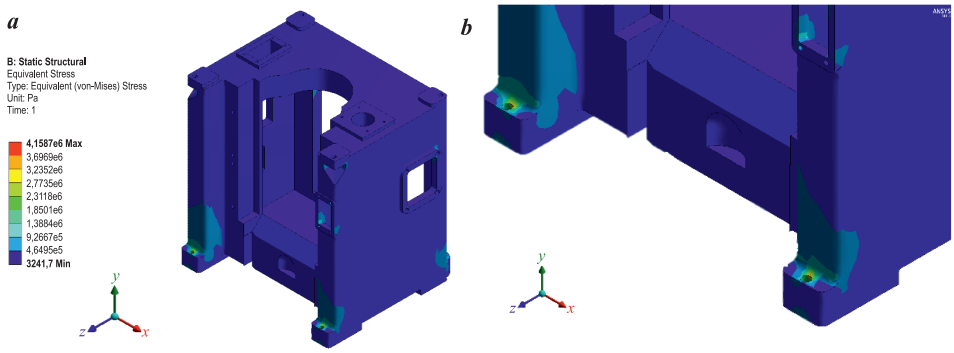

Fig. 8. Equivalent von Mises contour plot obtained for the critical load case of the housing model: a) overall view, b) area of maximum equivalent von Mises stress (detailed view)

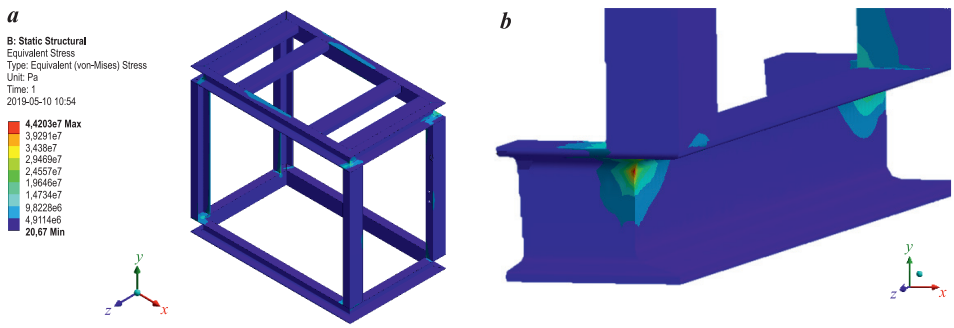

Fig. 9. Equivalent von Mises contour plot obtained for the critical load case of the frame model: a) overall view, b) area of maximum equivalent von Mises stress (detailed view)

In addition to the FEA tools available in ANSYS Workbench, tools for the Design and Analysis of Computer Experiments (DACE) were also used. A Central Composite Face-Centered Enhanced design was selected, as shown in Figure 10. The figure schematically illustrates the design points, of which there are 29 in total (three input parameters). Points $p_{1–8}$ and $p_{15–22}$ lie at the vertices of a conceptual cuboid, points $p_{9–14}$ and $p_{23–28}$ are located at the centers of its faces, and point p_{29} represents the center point of the design.

The optimization based on the selected input parameters was carried out using two different approaches: Response Surface Method with second-degree polynomial approximations and the Direct Optimization method. The objective function F_h for the commercially produced housing model is defined by Equations (3)–(6). In the case of the housing, the input parameters used in the optimization were: the thicknesses of the base, top, and rear walls of the model.

$$\min F_h(\eta) \Leftrightarrow \min F_h(x) \wedge \min F_h(m) \tag{3}$$

$$F_h(m) \leq 760 \text{ (kg)} \tag{4}$$

$$f_{h1}(\eta) \geq 60 \text{ (Hz)} \tag{5}$$

$$x(\eta) \leq 0.2 \text{ (mm)} \tag{6}$$

where:

η – vector of decision and output variables, consisting of maximum total deformation, mass of the housing and its fundamental natural frequency,
f_{h1} – the first (fundamental) natural frequency of the housing,
x – the maximum value of total deformation in the housing structure,
m – the mass of the housing.

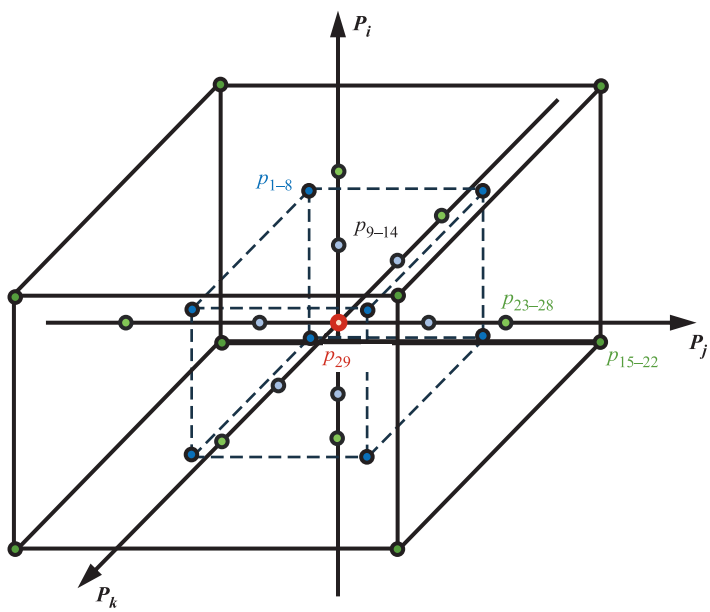

Fig. 10. Central Composite Face-Centered Enhanced design used in the DACE stage

The objective function F_f for the frame model is defined by Equations (7)–(12). In the case of the frame, the input parameters used in the optimization were the thickness of the profiles at the base, the thickness of the profiles at the top, and the thickness of the covers. An example of response surfaces based on second-order polynomial approximations is shown in Figure 11.

$$\min F_f(\eta) \Leftrightarrow \min F_f(x) \wedge \min F_f(m) \tag{7}$$

$$F_f(m) \leq 500 \text{ (kg)} \tag{8}$$

$$f_{f1}(\eta) \geq 44 \text{ (Hz)} \tag{9}$$

$$f_{f2}(\eta) \geq 60 \text{ (Hz)} \tag{10}$$

$$\sigma_{HMH}(\eta) \leq 117.5 \text{ (MPa)} \tag{11}$$

$$x(\eta) \leq 0.2 \text{ (mm)} \tag{12}$$

where:

η – vector of decision and output variables, consisting of: maximum total deformation, mass of the frame and its fundamental and second natural frequency,
f_{f1} – first natural frequency of the frame structure,
f_{f2} – second natural frequency of the frame structure,
σ_{HMH} – maximum equivalent von Mises stress in the frame model,
x – the maximum value of total deformation in the frame structure,
m – the mass of the frame.

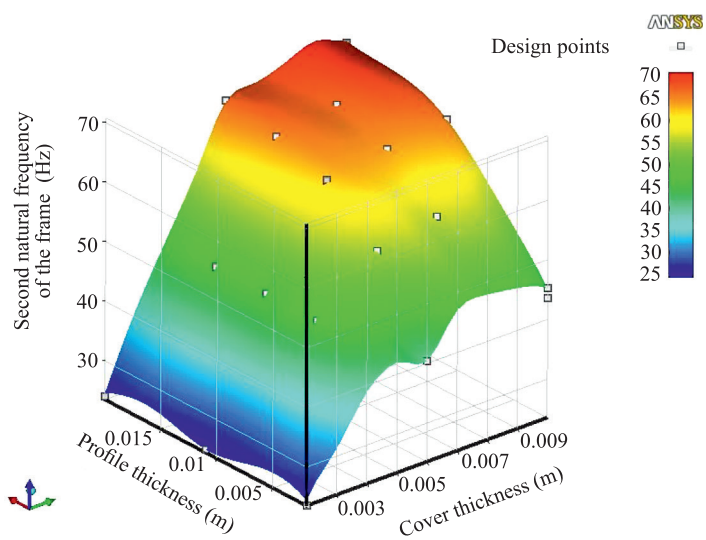

Fig. 11. Dependence of the second natural frequency on the thickness of the frame profiles and covers, illustrated by the response surface

Results

According to Table 5, it was necessary to adopt criteria that would ensure the greatest possible difference between the eigenfrequencies and the excitation frequencies – specifically, eigenfrequency values as far as possible from 30 Hz, 41.7 Hz, and 50 Hz. In the case of the housing model, preliminary simulations conducted prior to the optimization showed that the fundamental frequency was 54.7 Hz – only about 5 Hz above a "critical" excitation frequency. Moreover, the housing model exhibited very low von Mises equivalent stresses, approximately 4.2 MPa, along with a maximum total deformation of about 0.01 mm. As a result of the optimization process, these values were further reduced – to approximately 4.03 MPa and 0.005 mm using the response surface method, and to about 4 MPa and 0.0057 mm using the direct optimization method. Through the use of response surface-based optimization, the fundamental frequency of the housing model was increased to 61.25 Hz, while the direct method led to a first natural frequency of 60.171 Hz.

For the initial frame model, the first two natural frequencies were analyzed. Preliminary modal analysis showed that these frequencies were initially 30.04 Hz and 48.65 Hz. As a result of the optimization process, the corresponding values obtained using the response surface method and the direct method were 45.201 Hz and 46.108 Hz, and 67.679 Hz and 70.6 Hz, respectively. The initial values of von Mises equivalent stress and maximum total deformation were 60.036 MPa and 0.07 mm. Through response surface optimization, these were reduced to 38.3 MPa and 0.06 mm. With the direct method, they reached approximately 41.06 MPa and 0.06 mm. In both cases, the optimization process led to a reduction in these

Table 6

Results for housing and frame before and after optimization

for housing model	Initial model	Response Surface Optimization	Direct Optimization
Mass of the model m (kg)	620.06	736.83	713.28
Maximum total deformation u_{tot} (mm)	0.0088	0.005	0.0057
Maximum von Mises stress $\boldsymbol{\sigma}_{HMH}$ (MPa)	4.16	4.03	3.99
First natural frequency f_{h1} (Hz)	54.7	61.25	60.17
for frame model	Initial model	Response Surface Optimization	Direct Optimization
Mass of the model m (kg)	368.26	435.38	492.24
Maximum total deformation u_{tot} (mm)	0.07	0.0593	0.0606
Maximum von Mises stress $\boldsymbol{\sigma}_{HMH}$ (MPa)	60.04	38.3	41.06
First natural frequency f_{f1} (Hz)	30.04	45.2	46.11
Second natural frequency f_{f2} (Hz)	48.65	67.68	70.6

output quantities. The reduction in maximum von Mises stress in the frame model reached approximately 36% – a similar result for both optimization methods. Achieving these improvements was associated with an increase in the mass of the support structures. For the housing model, the mass increase for the response surface method and the direct method was 116.77 kg (18.83%) and 93.22 kg (15.03%), respectively. For the frame model, the increase amounted to 67.12 kg (approximately 18.2%) and 123.98 kg (33.67%). In this case, the response surface method achieved comparable benefits in terms of reduced equivalent stress and maximum total deformation, while keeping the total mass nearly 57 kg lower than with the direct method. The final results are summarized in Table 6.

Discussion

The results obtained for the two different support structures reveal significant differences. The machine with a cast iron housing exhibited a much greater mass – almost three times as heavy as the milling machine based on a steel frame. This was associated with better fulfillment of strength criteria. As shown in the preliminary analyses, both structures met the criteria for stiffness and structural strength. In the discussion of preliminary strength analyses, particular attention is given to model simplifications. Such simplifications enable more efficient determination of results for the analyzed numerical models, for example by replacing the influence of numerous smaller components of the structures under consideration, whose direct inclusion in the simulation would significantly increase computational demands due to the higher complexity of the FE models (necessity to model additional interactions between elements of the system, increased number of mesh nodes, more contact definitions, and longer model preparation times). The use of geometric simplifications aims to generate computational meshes with reduced node counts, and thus fewer degrees of freedom. The number of nodes can also be reduced by applying shell elements instead of solid elements, which are more demanding in terms of hardware resources. Simplifications in the form of boundary conditions that constrain degrees of freedom in the regions of supports are a standard procedure in FEM analyses. In the present case, such an approach was beneficial due to time constraints and the necessity to perform a large number of separate analyses within the undertaken optimization tasks. Although the computations could have been performed with more detailed modeling techniques, a compromise approach based on model simplifications was adopted, taking into account further optimization procedures and hardware limitations. Simulations with more advanced modeling of component connections, for instance using submodeling techniques, as well as the implementation of time-dependent dynamic effects such as tool vibrations or impact forces, may serve as a starting point for future design work, especially with the increasing capabilities of computing

stations and the growing accessibility of advanced numerical software such as ANSYS. The subsequent design efforts focused on modeling the natural vibrations in a way that would minimize the risk of resonance – particularly in the non-professional frame structure, where the first natural frequency nearly coincided with the operating frequency of the cutting tool. Future work may focus on incorporating additional machining-related phenomena such as fatigue wear or thermal effects. The selection of the material model could also be refined to reflect a more realistic, nonlinear structural response.

Conclusion

The obtained eigenfrequencies met the thresholds defined by the optimization criteria. For the housing, the target was a fundamental frequency of at least 60 Hz, while for the prototype frame model, the first and second natural frequencies were required to exceed 44 Hz and 60 Hz, respectively. In both cases, these objectives were achieved. Finite element analysis of the eigenfrequencies – particularly when combined with Design and Analysis of Computer Experiments (DACE) and optimization tools – enables preliminary verification of the structural design. For components used in machine tools, such verification is essential to ensure safe, reliable machining and adequate manufacturing precision. The conducted analyses demonstrate the advantages of the computational methods applied for determining the appropriate dimensions of support structures. Tools available in the ANSYS Workbench environment can be effectively used in the design of frames, housings, or even complete machines, supporting comprehensive simulation workflows. The simulations performed in this study also enabled a comparison of the proposed structural concepts.

While the legitimacy of such optimization efforts may be debated – especially given the simplified assumptions (assuming linear elastic material behavior) – there is no doubt that modal analysis remains a valuable design tool when selecting the dimensions of machine components using computer-aided engineering methods such as finite element techniques. Based on the adopted assumptions and mathematical models, with clearly defined optimization criteria, a preliminary design of machine components can be carried out so that the eigenfrequencies meet the specified threshold conditions while ensuring that structural strength requirements are satisfied.

Acknowledgement

This work was supported by the AGH University of Krakow, Faculty of Mechanical Engineering and Robotics, under subsidy no. 16.16.130.942.

References

CHAN T.-C., ULLAH A., ROY B., CHANG S.-L. 2023. *Finite element analysis and structure optimization of a gantry-type high-precision machine tool*. Scientific Reports, 13(1): 13006.

DIKMEN E., VAN DER HOOGT P., DE BOER A., AARTS R., JONKER B. 2009. *A Flexible Rotor on Flexible Supports: Modeling and Experiments*. Volume 15: Sound, Vibration and Design, 51-56.

DONG J., WANG G., LIN H., BI X., LI Z., ZHAO P., PEI T., TAN F. 2023. *Vibration Characteristic Analysis and Structural Optimization of the Frame of a Triplex Row-Baling Cotton Picker*. Agriculture, 13(7): 1440.

DUNAJ P., MARCHELEK K., CHODŹKO M. 2019. *Application of the finite element method in the milling process stability diagnosis*. Journal of Theoretical and Applied Mechanics, 57(2): 353-367.

GÉRADIN M., RIXEN D., FARHAT C. 2015. *Mechanical vibrations: Theory and applications to structural dynamics* (Third Edition). Wiley.

GOLI G., FIORAVANTI M., MARCHAL R., UZIELLI L., BUSONI S. 2010. *Up-milling and down- milling wood with different grain orientations – the cutting forces behaviour*. European Journal of Wood and Wood Products, 68(4): 385-395.

HERZ F., NORDMANN R. 2020. *Basics of Vibrations. Vibrations of Power Plant Machines* (pp. 1-28). Springer International Publishing.

JAROSZEWICZ J., ŁUKASZEWICZ K. 2018. *Analysis of natural frequency of flexural vibrations of a single-span beam with the consideration of Timoshenko effect*. Technical Sciences, 3(21): 215-232.

JAROSZEWICZ J., RADZISZEWSKI L., DRAGUN Ł. 2017. *The effect of influence of conservative and tangential axial forces on transverse vibrations of tapered vertical columns*. Technical Sciences, 4(20): 333-342.

JAROSZEWICZ J., ZORYJ L. 1994. *Transversal vibrations and stability of beams with variable parameters*. International Journal of Applied Mechanics and Engineering, 30(9): 713-720.

LIU J., KIZAKI T., REN Z., SUGITA N. 2022. *Mode shape database-based estimation for machine tool dynamics*. International Journal of Mechanical Sciences, 236: 107739.

PEDRAMMEHR S., FARROKHI H., RAJAB A. K. S., PAKZAD S., MAHBOUBKHAH M., ETTEFAGH M. M., SADEGHI M. H. 2011. *Modal Analysis of the Milling Machine Structure through FEM and Experimental Test*. Advanced Materials Research, 383-390, 6717-6721.

QIU M., WANG D., WEI H., LIANG X., MA Y. 2018. *Vibration modal analysis and optimization of the motor base*. MATEC Web of Conferences, 175: 03046.

SAWA M., SZALA M., HENZLER W. 2021. *Innovative device for tensile strength testing of welded joints: 3D modelling, FEM simulation and experimental validation of test rig – a case study*. Applied Computer Science, 17(3): 92-105.

SHIHAN M., CHANDRADASS J., KANNAN T. 2020. *Investigation of vibration analysis during end milling process of Monel alloy*. Materials Today Proceedings, 39: 695-699.

SZMIDLA J., KLUBA M. 2011. *Stateczność i drgania swobodne niepryzmatycznego układu smukłego poddanego obciążeniu eulerowskiemu*. Modelowanie Inżynierskie, 41: 385-394.

VERVAEKE R., DEBRUYNE S., VANDEPITTE D. 2019. *Numerical and experimental analysis of vibration damping performance of polyurethane adhesive in machine operations*. International Journal of Adhesion and Adhesives, 90: 47-54.

XI S., CAO H., CHEN X. 2019. *Dynamic modeling of spindle bearing system and vibration response investigation*. Mechanical Systems and Signal Processing, 114: 486-511.

ZIENKIEWICZ O. C., TAYLOR R. L. 2002. *The Finite Element Method: The Basis (Volume 1)*. Butterworth-Heinemann.